

ment of the ring give rise to an additional radial loading of intensity

$$q_n = N[(d^2w/ds^2) + (w/R^2)] = NM/EI \quad (8)$$

where  $M$  is the bending moment associated with the change in curvature due to the buckling. Treating expression (8) as a fictitious radial loading, equilibrium of the ring in the buckled form can be studied on the basis of Eq. (6), which for this case becomes

$$(d^2M/d\theta^2) + M = -R^2 MN/EI \quad (9)$$

$N$  now being considered positive when it represents compression. Introducing the notation

$$n^2 = 1 + (R^2N/EI) \quad (10)$$

we can write Eq. (9) in the condensed form

$$d^2M/d\theta^2 + n^2M = 0 \quad (9a)$$

To illustrate the use of Eq. (9a) in studying the stability of a uniformly compressed circular ring, consider the sector hinged at its ends  $A$  and  $B$  and subtending a central angle  $2\alpha$  as shown in Fig. 2. In the circular solid line configuration, this ring is in equilibrium under the action of a uniform radial load of intensity  $q = -p$  (not shown) and carries a corresponding uniform axial compression  $N = pR$ . To test whether this equilibrium configuration is stable or unstable, we superimpose an inextensional bending deformation, as shown by the dotted line  $AB$ , and use Eq. (9a). The general solution of this equation is

$$M = A \cos n\theta + B \sin n\theta \quad (11)$$

where  $A$  and  $B$  are constants. For the hinged ends of the sector, we have  $M = 0$  when  $\theta = \pm\alpha$ . With these boundary conditions, Eq. (11) gives

$$0 = A \cos n\alpha + B \sin n\alpha \quad (12)$$

$$0 = A \cos n\alpha - B \sin n\alpha$$

or, more simply,

$$A \cos n\alpha = 0 \quad B \sin n\alpha = 0 \quad (13)$$

For inextensional buckling, we take  $A = 0$  and  $B \neq 0$ . Then, for equilibrium in the buckled form, we must have

$$\sin n\alpha = 0$$

which yields the eigenvalues

$$n = m(\pi/\alpha) \quad (14)$$

where  $m$  is an integer. Returning to Eq. (10), we conclude this to mean that the critical value of the compressive force in the ring is

$$N_{cr} = [m^2(\pi^2/\alpha^2) - 1](EI/R^2) \quad (15a)$$

or, correspondingly, that the critical radial loading is

$$p_{cr} = [m^2(\pi^2/\alpha^2) - 1](EI/R^3) \quad (15b)$$

Taking the integer  $m = 1$ , we obtain the lowest critical values from (15a) and (15b).

In the case of a uniformly compressed full ring, we have  $\alpha = \pi$  and Eqs. (15) become

$$N_{cr} = (m^2 - 1)(EI/R^2) \quad (16a)$$

$$p_{cr} = (m^2 - 1)(EI/R^3) \quad (16b)$$

In this case the integer  $m = 1$  corresponds to a rigid body displacement of the ring, and the lowest buckling load is obtained by taking  $m = 2$ .

The results represented by Eqs. (15) and (16) are well known<sup>1</sup> but have always been obtained on the basis of Eq. (7). The purpose of this note is simply to call attention to

the equilibrium equation (6) and its application in the treatment of curved bars. It is possible that a similar approach to other problems involving curved bars and shells might prove useful.

#### References

- Timoshenko and Gere, *Theory of Elastic Stability* (McGraw-Hill Book Co., Inc., New York, 1961), 2nd ed., pp. 289, 291, and 297.

## Oblique Injection of a Jet into a Stream

LU TING\* AND CHARLES J. RUGER†

*Polytechnic Institute of Brooklyn, Farmingdale, N. Y.*

THE problem of a jet injected obliquely at an angle  $\alpha$  ( $\pi > \alpha > 0$ ) into a uniform stream can be used as a simple model to simulate many engineering problems, namely, the wing fan, the ground effect machine, etc. When the flow is assumed to be incompressible and inviscid, the jet will be bent by the main stream and will be bounded by two streamlines. They are the free streamline, which separates the jet from the wake behind it, and the interface, which separates the jet from the main stream (Fig. 1a). With the upstream uniform velocity  $U_\infty$  and the width of the jet  $b$  as the scales for velocity and length, respectively, the solutions of the problem will depend only on the dimensionless parameter  $\kappa$ , which is defined as  $(P_j - P)/(\frac{1}{2}\rho U_\infty^2)$ , where  $P_j$  and  $P$  are the total pressure for the jet and the main stream, respectively. For example, the inclination of a streamline  $\theta$  can be written, in general, as  $\theta = \theta(x, y, \kappa)$ . Here, the pressure in the wake has been assumed to be equal to the pressure at upstream infinity. Otherwise, the solution would also depend on the cavitation number.

When the jet and the main stream have the same total pressure, i.e.,  $\kappa = 0$ , the velocity magnitude  $q$  and the inclination  $\theta$  are continuous along the interface, and the potential solution for the jet and that for the main stream are therefore analytic continuations of each other. An analytic solution for both the jet and the main stream can be obtained by the standard technique for free streamline problems.<sup>1</sup> Figures 1b and 2a show, respectively, the complex potential  $\chi$  plane,  $\chi = \varphi + i\psi$ , and the complex conjugate velocity  $w$  plane,  $w = qe^{-i\theta}$ . They are self-explanatory with the exception of the segment  $BC$  in the  $x$  plane which corresponds to the opening of the jet. We assume that the jet is louvered so that the flow direction may be specified, and thus the segment  $BC$  in the  $x$  plane obeys the condition

$$\left. \frac{d\psi}{d\varphi} \right|_{y=0} = \left( \frac{\partial\psi/\partial x}{\partial\varphi/\partial x} \right)_{y=0} = - \left( \frac{v}{u} \right) = -\tan\alpha \quad 0 < x < 1$$

Hence, it is a straight line in the  $x$  plane inclined at an angle  $-\alpha$ . The standard technique is to map the circular sector in the  $w$  plane to the upper half plane and then to the open polygon in the  $x$  plane. Then the conformal mapping function  $w(x)$  which can be obtained readily<sup>2</sup> can be used to relate  $x$  to  $z$  by the integral  $z = \int dx/w$ . The unknown constant  $\psi_j$  will then be related to the width of the jet  $b$ .

For the case  $\kappa \neq 0$ , the pressure across the interface has to be continuous; therefore, there is a discontinuity in the magnitude of velocity. The discontinuity is defined by Ber-

Received September 4, 1964. This research was supported by the U.S. Army Transportation Command under Contract No. DA 44-177-AMC-91(T).

\* Research Professor of Aerospace Engineering; now Professor of Aeronautics and Astronautics, New York University, New York, N.Y. Member AIAA.

† Research Fellow; now Assistant Research Scientist, New York, N. Y.

noulli's equation. The solution in the jet and that in the main stream cannot be analytic continuations of each other. The standard method of conformal mapping from the complex potential plane to the conjugate velocity plane will not be fruitful because the line separating the jet and the main-stream is mapped into two unknown curves in the conjugate velocity plane (Fig. 2b and Fig. 2c). For the special case of  $\alpha = 90^\circ$ , the problem has been reduced to two nonlinear singular integral differential equations in Ref. 3. Attempts at a numerical solution of these two equations for any value of  $\kappa > 0$  have not been successful.

It would appear natural to solve for the limiting case of small  $\kappa$  by the method of small perturbation from the known solution of  $\kappa = 0$ . It is the purpose of this note to point out that the solution for small  $\kappa$  will not approach the solution of  $\kappa = 0$  uniformly.

In particular, it will be shown that the inclination of the interface ( $\psi = 0, \varphi > 0$ ) at the opening of the jet ( $x = 0, y = 0$  or  $\psi = 0$  and  $\varphi = 0^+$ ) is a discontinuous function of  $\kappa$  at  $\kappa = 0$ , namely,

$$\theta(\psi = 0, \varphi = 0^+, \kappa > 0) = \alpha \quad (1)$$

$$\theta(\psi = 0, \varphi = 0^+, \kappa = 0) = [\pi\alpha/(\pi + \alpha)] \quad (2)$$

$$\theta(\psi = 0, \varphi = 0^+, -1 < \kappa < 0) = 0 \quad (3)$$

although the values of  $\theta$  along  $y = 0$  are specified, i.e.,

$$\theta(y = 0^+, x < 0, \kappa) = 0 \quad (4)$$

$$\theta(y = 0^+, 0 < x < 1, \kappa) = \alpha \quad (5)$$

for any  $\kappa > -1$ .

In this note, the results of Eqs. (1-3) will be derived by utilizing the local properties of the potential solutions<sup>4, 5</sup> without obtaining the complete solutions.

Since the streamline  $\psi = 0, \varphi < 0$  of the main stream intersects the streamline from the jet at angle  $\alpha$ , at least one of the streamlines has to form a concave corner with the interface ( $\psi = 0, \varphi > 0$ ). The properties of a potential flow in a concave corner require that the corner be a stagnation point and that the flow cannot make a sharp turn with finite velocity.<sup>4</sup>

For  $\kappa > 0$ , i.e., the jet has a higher stagnation pressure, the maximum pressure along the interface can be only the stagnation pressure of the main stream. Hence, the jet will have a finite velocity at the point  $y = 0, x = 0^+$ , and the inclination of the interface at that point has to be the same as the direction of the jet. Thus, Eq. (1) is valid. Simi-

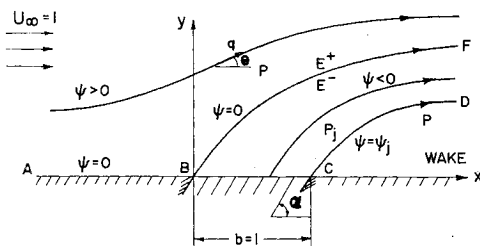


Fig. 1a Physical plane ( $z = x + iy$ ).

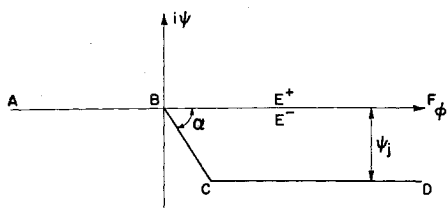


Fig. 1b Complex potential plane ( $\chi = \phi + i\psi$ ).

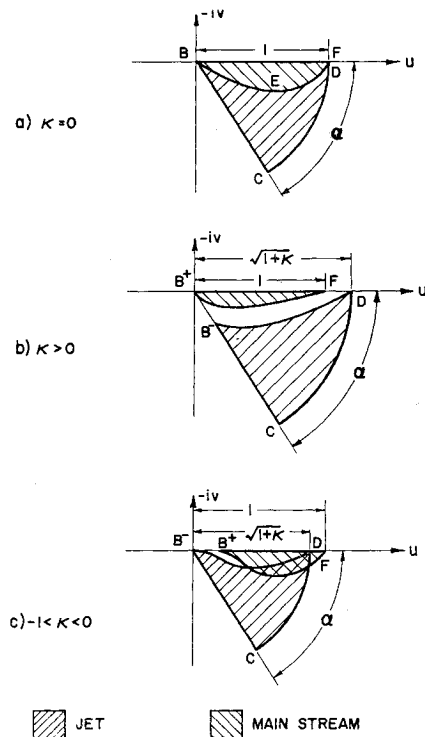


Fig. 2 Complex conjugate velocity plane ( $w = u - iv = qe^{-i\theta}$ ).

larly, for  $\kappa < 0$ , the velocity of the main stream at the point  $x = 0^-, y = 0$  is finite, and Eq. (3) becomes valid.

For  $\kappa = 0$ , both the jet and the main stream have the same stagnation pressure. If either one of them makes a sharp turn as the pressure reaches the common stagnation pressure, the other one can also make a sharp turn. Hence, the fore-mentioned property of potential flow will not define the angle  $\theta(\psi = 0, \varphi = 0^+, \kappa = 0)$ . The following additional property of potential flow has to be introduced.<sup>5</sup>

Since  $\theta$  is a potential function of  $x, y$  subject to the boundary condition with a jump along  $y = 0$  at  $x = 0, y = 0$ , as defined by Eqs. (4) and (5), the limit of  $\theta$  as  $x \rightarrow 0, y \rightarrow 0$  will depend on the direction of the path in the following manner:

$$\lim_{x \rightarrow 0, y \rightarrow 0} \theta(x, y) = \frac{(\alpha/\pi)[\pi - \arctan y/x]}{\arctan y/x = \text{const}} \quad (6)$$

Along the direction of the interface,  $\theta(\psi = 0, \varphi = 0^+) = \arctan(y/x)$ , and Eq. (6) yields Eq. (2), i.e.,  $\theta(\psi = 0, \varphi = 0^+) = [\pi/(\pi + \alpha)]\alpha$ .

An alternate proof of Eq. (2) can be obtained by considering  $\theta$  as a potential function of  $\varphi$  and  $\psi$  with the boundary conditions that  $\theta = 0$  along  $AB$  and  $\theta = \alpha$  along  $BC$  (see Fig. 1b). The limit of  $\theta$  as  $\varphi$  and  $\psi$  approach zero again depends on the direction of the path in a similar manner<sup>5</sup> as Eq. (6):

$$\lim_{\varphi \rightarrow 0^+, \psi \rightarrow 0} \theta(\varphi, \psi) = \frac{[\alpha/(\pi + \alpha)][\pi - \arctan(\psi/\varphi)]}{\arctan(\varphi/\psi) = \text{const}}$$

It reduces to Eq. (2) along the line  $\arctan(\psi/\varphi) = 0$ .

In Ref. 3, the exact solution with  $\kappa = 0$  is obtained by conformal mapping for the special case of  $\alpha = 90^\circ$ . The result is in agreement with Eq. (2). A numerical scheme for the special case of small positive  $\kappa$  and  $\alpha = 90^\circ$  is also presented in Ref. 3.

Since the derivations depend only on the local properties, Eqs. (1-3) will be valid not only for any value of  $\alpha$  between 0 and  $\pi$ , but also, for any cavitation number.

References

- <sup>1</sup> Birkhoff, G. and Zarantonello, E. H., *Jets, Wakes, and Cavities* (Academic Press, Inc., New York, 1957).
- <sup>2</sup> Churchill, R. V., *Complex Variables and Applications* (McGraw-Hill Book Co., Inc., New York, 1960), 2nd ed.
- <sup>3</sup> Ting, L., Libby, P. A., and Ruger, C., "The potential flow due to a jet and a stream with different total pressures," Polytechnic Institute of Brooklyn, PIBAL Rept. 855 (August 1964).
- <sup>4</sup> Prandtl, L. and Tietjens, O. G., *Fundamentals of Hydro- and Aeromechanics* (Dover Publications, Inc., New York, 1934).
- <sup>5</sup> Nehari, Z., *Conformal Mapping* (McGraw-Hill Book Co., Inc., New York, 1952).

## Extension of Reaction Control Effectiveness Criteria to Mach 10: Experiment and Theory

PAUL W. VINSON\*  
*Martin Company, Orlando, Fla.*

**R**EACTION control experiments at supersonic speeds have shown that control forces significantly greater than the jet reaction force can be generated in atmospheric flight.<sup>1-7</sup> Data of Ref. 2 indicate that two-dimensional reaction control effectiveness can be obtained on bodies of revolution by employing fixed, low-aspect-ratio fins to retard circumferential propagation of the upstream separated flow. Theories have been advanced by several investigators<sup>1-5</sup> which indicate the beneficial effects of increased flight Mach numbers. However, available experimental data have not covered a wide enough Mach number range to establish conclusively the Mach number influence.

The purpose of this note is to present experimental data on reaction control effectiveness at Mach 6 and 10. Tests were conducted at the Naval Ordnance Laboratory, Silver Spring, Md., in tunnel no. 8 and employed a body-of-revolution model with fins as shown in Fig. 1. A cold air jet, consisting of a sonic slot spanning the body circumference between adjacent fins, was utilized. Slot width was 0.015 in. and the slot was located 0.25 in. from the model base. Force balance as well as body pressure data were obtained at all test points, and a turbulent boundary layer was obtained by mounting a 0.015-in.-diam wire on the model nose.

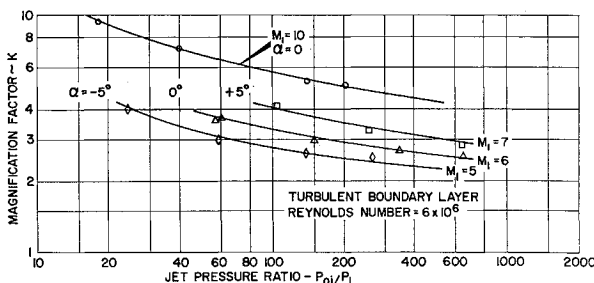
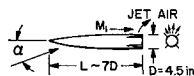


Fig. 1 Experimental magnification factors at hypersonic Mach numbers.

Experimental Data

Figure 1 indicates the influence of Mach number and jet pressure ratio on the jet magnification factor where the magnification factor is defined as the ratio of body plus reaction force to reaction force. Model angle of attack was varied to  $\pm 5^\circ$  at Mach 6 providing local Mach numbers of 5 and 7. These data clearly show the improved effectiveness at hypersonic Mach numbers.

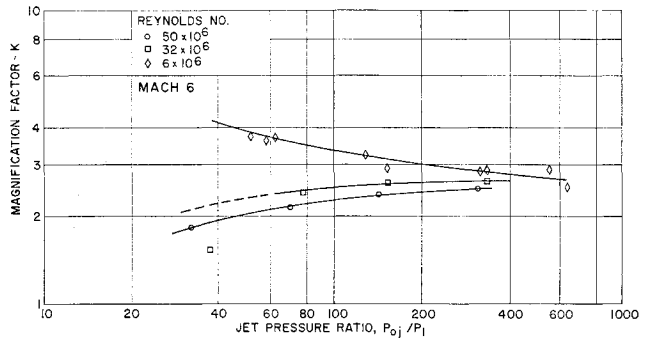


Fig. 2 Effect of Reynolds number on magnification factor.

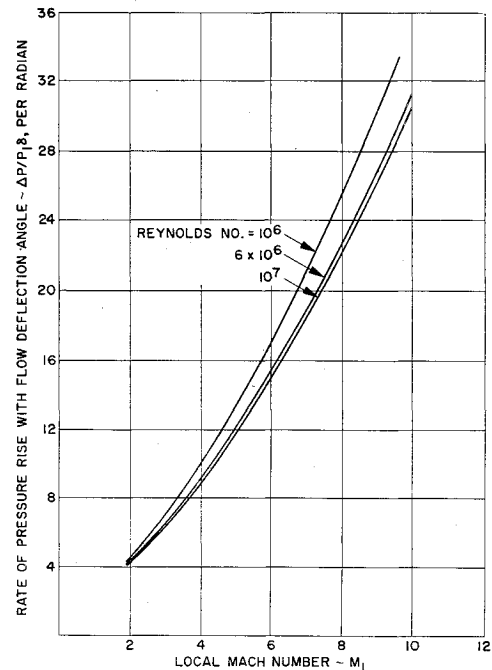


Fig. 3 Turbulent boundary-layer separation.

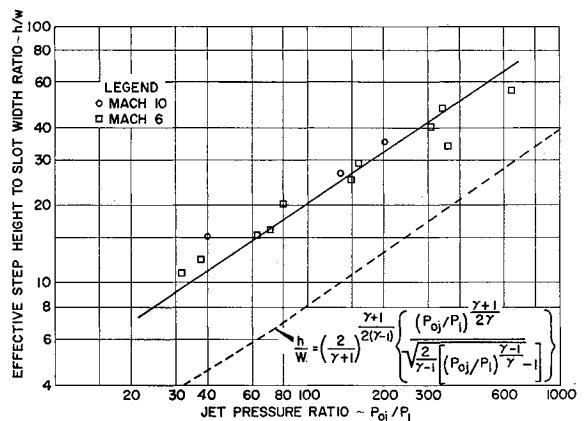


Fig. 4 Correlation of jet penetration data.

Received September 8, 1964. This research was sponsored by the Advanced Research Projects Agency, Department of Defense, and is a part of Project DEFENDER.

\* Design Engineer. Member AIAA.